Laser Light Scattering Study of Pressure-Induced Micellization of a Diblock Copolymer of Poly(1,1-dihydroperfluorooctylacrylate) and Poly(vinyl acetate) in Supercritical Carbon Dioxide

Shuiqin Zhou and Benjamin Chu*

Department of Chemistry, State University of New York at Stony Brook, Long Island, New York 11794-3400

Received February 20, 1998; Revised Manuscript Received May 26, 1998

ABSTRACT: Laser light scattering has been employed to study the pressure-induced associating behavior of a diblock copolymer of poly(1,1-dihydroperfluorooctylacrylate) and poly(vinyl acetate) (PFOA-*b*-PVAC) in supercritical carbon dioxide, a pressure-dependent selective good solvent for the PFOA block. Over a pressure range of 90−552 bar at 65 °C, as can be observed experimentally, there exist five pressure regions. At very low pressures (<148 bar), the PFOA-*b*-PVAC copolymer is essentially insoluble in pressurized carbon dioxide. At low pressures (148−206 bar), a small portion of the copolymer is dissolved to form unimers with a constant average hydrodynamic radius $\langle R_h \rangle$ of about 2.2 nm. Around a phase separation pressure of ∼225 bar, most of the copolymers were dissolved to form unimers in solution. In the pressure region of 242−310 bar, micelles with a very narrow size distribution were formed in equilibrium with single polymer chains (or unimers). In the high-pressure region (i.e., 379−552 bar), the micelles were gradually dissolved to unimers with increasing pressure, while some anomalous large aggregates appeared around the critical micelle pressure. The appearance of the anomalous larger aggregates can be ascribed to the copolymer composition heterogeneity. On the basis of a model of the mass action law of micelle formation and the bimodal size distribution obtained by the CONTIN analysis, quantitative information such as the critical micelle concentration (cmc), and the average association number (N) were estimated in the normal micellar region. With increasing pressure, the cmc increased, but N decreased. The kinetics of dissolution and of micelle formation of the copolymer around the phase separation pressure region was also examined.

Introduction

Supercritical carbon dioxide is rapidly becoming an attractive alternative to a variety of organic solvents for use in analytical processes, polymer manufacturing, and pharmaceuticals since it is viewed as an environmentally benign medium to minimize waste and to reduce volatile organic emissions.[1−5] Not only is supercritical CO_2 more environmentally acceptable, but it is also nontoxic, nonflammable, and naturally abundant and has an easily accessible critical point ($T_c = 31$ °C, $P_c = 73.8$ bar). However, only two classes of polymeric materials, silicones and highly fluorinated polymers, have been shown to exhibit significant solubility in supercritical CO_2 under relatively moderate conditions ($T < 100$ °C, and $P < 500$ bar),[6−9] although many nonionic, low molar mass organics are soluble in liquid and supercritical CO_2.[6,10] In terms of the solubility of polymers in CO_2, we categorize the amorphous fluorinated polymers and silicon polymers into "CO_2-philic", while conventional polymers, either hydrophilic or lipophilic, are relatively insoluble in CO_2, and are termed "CO_2-phobic".

In the past few years, some block copolymers designed specifically to be amphiphilic in supercritical CO_2 have been synthesized.[1,8] It was anticipated that these amphiphilic block copolymers would self-assemble into micelles consisting of a CO_2-phobic core and a CO_2-philic corona when dissolved in supercritical CO_2. Such types of block copolymers could serve as surfactants to sterically stabilize the colloidal system for emulsion polymerization of CO_2-phobic monomers or separation of CO_2-phobic materials in supercritical CO_2.

In general, block copolymers form micelles in selective solvents that are thermodynamically good solvents for one type of block but are nonsolvents (or poor solvents) for the other type of block. The self-assembly of block copolymer chains in solution can usually be initiated either by an increase in concentration via the critical micelle concentration (cmc) or by changing the temperature via the critical micelle temperature (cmt). The cmc is defined as the copolymer concentration, above which the formation of micelles becomes increasingly important. The cmt is the transition temperature, above or below which the formation of associated structures becomes appreciable. In our laboratory, we have performed a series of studies on the temperature-induced micellization of various block copolymers with different composition and chain architecture.[11−15] The mechanism behind this can be ascribed to the considerable modification of the selective solvent quality characteristics for the block copolymers by changing the temperature. Analogously, supercritical fluids have a key advantage that the solvent quality for the block copolymers can be manipulated by simply changing the pressure of the system. In other words, the CO_2-philic/CO_2-phobic characteristics of the block copolymers in supercritical CO_2 can be modified by adjusting the pressure. Thus, the micelle formation, the micelle size, and the micelle breaking-up can be controlled by changing the pressure. Being able to vary the micelle size should be extremely useful because it might allow industrial chemists to influence reactions occurring inside the micelles. By breaking up the micelles, chemists could be able to cause whatever is inside the micellar microreactors to drop out of the solution. A

S0024-9297(98)00262-9 CCC: $15.00
Published on Web 07/21/1998

better understanding on the self-assembly behavior of these CO_2-amphiphilic polymers in supercritical CO_2 is of primary importance for quantifying their growing role in polymer synthesis and processing using supercritical fluids.

Laser light scattering (LLS) is a powerful technique for probing various types of molecular aggregates in the submicrometer size range. Static light scattering (SLS) can offer similar types of information as small-angle X-ray scattering (SAXS) and small angle neutron scattering (SANS), while dynamic light scattering (DLS) can provide us information on the translational diffusion coefficient (D), the hydrodynamic radius (R_h), and the particle size distribution in terms of R_h. In a mixture of unimers (u) and micelles (m), the intensity contributions (I_u and I_m) coming from a bimodal size distribution, together with the association number, can provide us an estimation of weight fractions of unimer and micelle species. Moreover, LLS is more available in academic or industrial laboratories in comparison with SAXS or SANS.

So far, many SAXS and SANS studies on the molecular dissolution/aggregation behavior of surfactants or polymers in supercritical fluids have been reported.[9,16−23] However, only a few LLS studies have been carried out in supercritical fluids.[24−26] One reason is probably due to the experimental difficulties in the ability to construct suitable light transmitting windows under fairly high pressures. Fulton and co-workers have studied the microemulsions of small surfactant molecules in supercritical light alkanes or xenon by LLS.[24−26] The problem is that the thick sapphire cell window could depolarize the incident laser beam. The Hasimoto group has recently reported a two-window high-pressure LLS cell with a large-size optical isotropic quartz glass (40-mm thickness) as one of the two windows.[27] However, due to the brittleness of quartz glass, such an LLS cell can only be operated in the mid-high-pressure range up to about 340 bar, which is not sufficient for the study of many supercritical fluid systems. Another reason is due to the low light scattering contrast between the solute and the supercritical carbon dioxide. For example, the refractive index increment of fluorinated polymers in CO_2 is very small. Very recently, we have constructed a new high-pressure fiber-optic LLS spectrometer with gradient index of refraction microlenses as cell windows.[28] The use of the fiber-optic probes not only miniaturized the LLS spectrometer, but also provides a high spatial coherence factor (β) value of 0.7−0.9.[28,29] With this high β value, we were able to carry out DLS experiments with a high signal-to-noise ratio.

In this paper, we report some LLS results on the pressure-induced self-assembly behavior of a diblock copolymer of poly(1,1-dihydroperfluorooctylacrylate) and poly(vinyl acetate) (PFOA-*b*-PVAC) in supercritical CO_2 by using our high-pressure fiber-optic LLS spectrometer. To our knowledge, this is the first LLS study on the molecular association of a block copolymer in supercritical CO_2. The equipment has proven to be very useful in probing the self-assembly behavior of block copolymers in supercritical CO_2, especially for large aggregates over 100 nm which have a length scale beyond the conventional SAXS or SANS experiments. The size, the size distributions, the intensity contributions from each species, and the quantitative calculation based on the CONTIN analysis provide us further information on the pressure-induced molecular association process of the diblock copolymer in supercritical CO_2. Such studies should aid us in the development of new routes for polymer synthesis or processing in this relatively benign solvent.

Experimental Section

Materials. SFC grade CO_2 for the LLS experiments was purchased from Scott Specially Gases. α,α,α-trifluorotoluene (Aldrich, 99 +%) was used as received. Vinyl acetate (VAC, Aldrich) and 1,1-dihydroperfluorooctylacrylate (FOA, 3 M) were purified and deinhibited by passage through an alumina column and was deoxygenated by argon purge prior to use. Benzyl *N*,*N*-diethyldithiocarbamate (BDC) was synthesized according to previously published literature.[7]

Synthesis of the PFOA-*b*-PVAC Diblock Copolymer. The block copolymer was synthesized using the iniferter polymerization technique by first polymerizing PVAC block using BDC as the iniferter in conjuction with UV light.[30] After the PVAC block was purified and characterized, it was dissolved and reacted with the second monomer. The produced block copolymer was then purified by soxhlet extraction. The diblock copolymer used in this paper was obtained from Professor J. M. DeSimone at UNC at Chapel Hill. The sample had molecular weight of 4.31×10^4 g/mol for the PFOA block, and 1.03×10^4 g/mol for the PVAC block, respectively. The PVAC block had a polydispersity of $M_w/M_n = 1.6$.

High-Pressure Fiber-Optic LLS Instrumentation. The details of the instrumentation and its principles can be found elsewhere.[28] Briefly, the homemade high-pressure LLS cell was machined from 316 stainless steel. Besides the incident and exit windows, three detectable windows were opened giving access to 30, 90, and 150° scattering angles. Single or multiple fiber-optic probes, each comprising of an optical fiber and a graded index microlens, are used to transmit the incident laser beam and to receive the scattered light from the high-pressure cell. Our fiber-optic probes positioned at different angles form an integral part of the scattering cell. Thus, no transparent windows and no goniometer are required. Such an arrangement has enabled us to use the microlens itself as the optical window in the high-pressure cell for LLS measurements. In the present setup, single fiber optic probes were used at 90 and 150°, while a multiple fiber optic probe with six fibers was used at 30°. The calibrated results for all eight of the fiber probes are located at 27.6°, 29.1°, 30.7°, 32.0°, 33.6°, 35.7°, 94.0°, and 146°, respectively. The total sample chamber volume could be varied from 2.4 to 6.0 mL. The inside surface of the cell was blackened to prevent light reflection. The sample in the cell could be stirred with a 12 × 7 mm, Teflon-coated magnetic stirring bar while the cell was put on the stirring plate. Pressure inside the cell was monitored by using a OMEGADYNE pressure transducer (TH-1) with a gauge meter (INFS-0001-DC1). The temperature of the cell was controlled by an OMEGA temperature controller (MODEL CN-76000) equipped with four OMEGA CSS cartridge heaters and a platinum RTD probe (PR-13).

High-Pressure LLS Measurements. A Spectra-Physics Model 165 argon ion laser operated at 488 nm was used as the light source. The PFOA-*b*-PVAC diblock copolymer used for high-pressure LLS measurements was dust-freed as follows. First, it was dissolved in α,α,α-trifluorotoluene at 2×10^{-3} g/mL and then filtered carefully into a dust-free bottle by using 0.2 μm Millipore filters; finally, the solution was evaporated and vacuum-dried at 45 °C for 1 week. The high-pressure cell was dust-freed by flowing filtered supercritical CO_2 through the sample chamber for 1 h before use. A known amount of sample was added to the high-pressure cell from the exit window channel. After having heated the cell to the desired temperature, it was pressurized with CO_2 to the desired pressure. The light-scattering measurements were recorded after the solution had been stirred for 1−10 h and further equilibrated for 5−10 h, both depending on the working pressure. Experiments were typically performed with pressure and temperature accuracies of ±0.5 bar and ±0.2 °C, respectively. Photon correlation measurements were carried out in

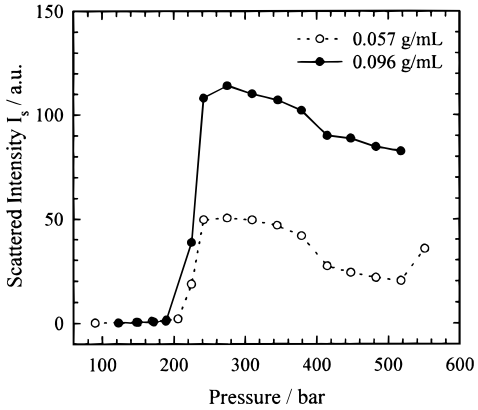

Figure 1. Plots of excess scattered intensity (measured at $\theta = 32°$, and $T = 65$ °C in arbitary units) vs pressure for the PFOA-*b*-PVAC copolymer in supercritical CO_2 at concentrations of 0.057 and 0.096 g/mL, respectively.

the self-beating mode by using a Brookhaven Instruments digital correlator (BI9000). The collected data were analyzed by using the CONTIN program[31] to extract information on the distribution of characteristic relaxation rates or the average hydrodynamic size, respectively.

Results and Discussion

Scattered Light Intensity vs Pressure. In general, the micelle formation can be initiated by an increase in concentration via the cmc or by changing the temperature via the cmt. Similarly, for a fluorinated block copolymer in supercritical CO_2, the molecular association process can be studied via the pressure dependence of the scattered intensity or the hydrodynamic size (distribution) of the particles in solution. Figure 1 shows the pressure dependence of the excess scattered intensity measured at a scattering angle of 32° for the PFOA-*b*-PVAC copolymer solution and at two different concentrations of 0.057 and 0.096 g/mL, respectively. Here the excess scattered intensity is defined as the difference in the scattered intensity between the solution and the supercritical CO_2 solvent. Both of the curves show five regions. (1) At very low pressures (<148 bar), nearly no excess scattered intensity was detected even though the refractive index difference between the copolymer and the solvent Δn ($\Delta n = n_p - n_s$, where n_p and n_s represent the refractive index of the copolymer and that of the solvent, respectively) was sufficiently large (>0.9) to detect the excess scattered intensity if enough solute were present. The result indicated that the copolymer did not dissolve in supercritical CO_2 at such low pressures. (2) At low pressures (148−206 bar), very low excess scattered intensity was detected; meanwhile, the scattered intensity increased slightly with increasing pressure. No appreciable difference was observed for the two solutions at different concentrations. The results suggest that in this low-pressure region, a small portion of the copolymer chains started to be dissolved when the solvent quality became better with increasing pressure. (3) When the pressure was increased from 206 to 242 bar, the Δn value changed from +0.015 to −0.015. Although the Δn values were very small, the scattered intensity increased dramatically. As will be discussed later, the block copolymers started to be dissolved in this range and micelles were formed at 242 bar. (4) At moderate pressures (242−379 bar), Δn changed from −0.015 to −0.077 continuously when pressure was increased from 242 to 379 bar. In principle, the scattered intensity should increase by a factor of about 20. However, with increasing pressure, the detected scattered intensity decreased slightly. The decrease in the scattered intensity was due to the increase in cmc and the decrease in the aggregation number of micelles caused by the better solvent quality for the copolymer with increasing pressure. (5) At high pressures (> 379 bar), the scattered intensity first decreased sharply to about 415 bar and then decreased very slowly until it reached 518 bar. In principle, with increasing pressure, the supercritical CO_2 becomes a better solvent for both PFOA and PVAC blocks, which leads to a gradual dissolution of micelles; thus, the scattered intensity should decrease. However, Δn increased from −0.077 to −0.11 when pressure was increased from 379 to 518 bar, which could introduce an increase in the scattered intensity by a factor of about 2. For the solution with concentration of 0.057 g/mL, the scattered intensity increased when pressure was increased from 518 to 552 bar although the Δn increase was very small (from −0.115 to −0.121). As will be evidenced by DLS later, this increase in the scattered intensity was due to the appearance of some anomalous large aggregates when the pressure was close to the critical micelle pressure under the measured concentration and temperature.

Hydrodynamic Radius Distributions vs Pressure. In dynamic light scattering, the precise intensity−intensity time correlation function $G^{(2)}(t,q)$ in the self-beating mode has the form[32,33]

$$G^{(2)}(t,q) = A[1 + \beta|g^{(1)}(t,q)|^2] \quad (1)$$

where $q = (4\pi n/\lambda)\sin(\theta/2)$ with n, λ, and θ being the solvent refractive index, the wavelength of light in vacuo, and the scattering angle, respectively, A is a measured baseline, β, a constant depending on the coherence of detection, t, the delay time, and $g^{(1)}(t,q)$, the normalized electric field time correlation function

$$g^{(1)}(t,q) = \int_0^\infty G(\Gamma)e^{-\Gamma t}\,d\Gamma \quad (2)$$

with $G(\Gamma)$ being the normalized line width distribution function at infinite dilution. As $q \to 0$, the line width (or relaxation rate) Γ can be expressed as $\Gamma/q^2 = D$ with D being the translational diffusion coefficient. $G(\Gamma,q)$ can be obtained from the Laplace inversion of the measured $G^{(2)}(t,q)$.[31] After learning the D value, we can further determine the (equivalent) hydrodynamic radius R_h by using the Stokes−Einstein relation

$$R_h = k_B T/6\pi\eta D \quad (3)$$

where k_B is the Boltzmann constant, and η is the solvent viscosity. It should be mentioned that both n and η[34] are pressure dependent in supercritical CO_2. In the present work, n is calculated by using the equation[35]

$$V\frac{n^2-1}{n^2+2} = 6.600 + \frac{1.25}{V} - \frac{264}{V^2} \quad (4)$$

where $V = M/\rho$ in mL/(g·mol) with M and ρ being the molar mass and the density of CO_2, which can be found elsewhere.[36]

Figure 2 shows the hydrodynamic radius distributions over a pressure range of 148−552 bar for the PFOA-*b*-PVAC diblock copolymer solution with $C = 0.057$ g/mL at $\theta = 32°$, and $T = 65$ °C. The intensity contribution

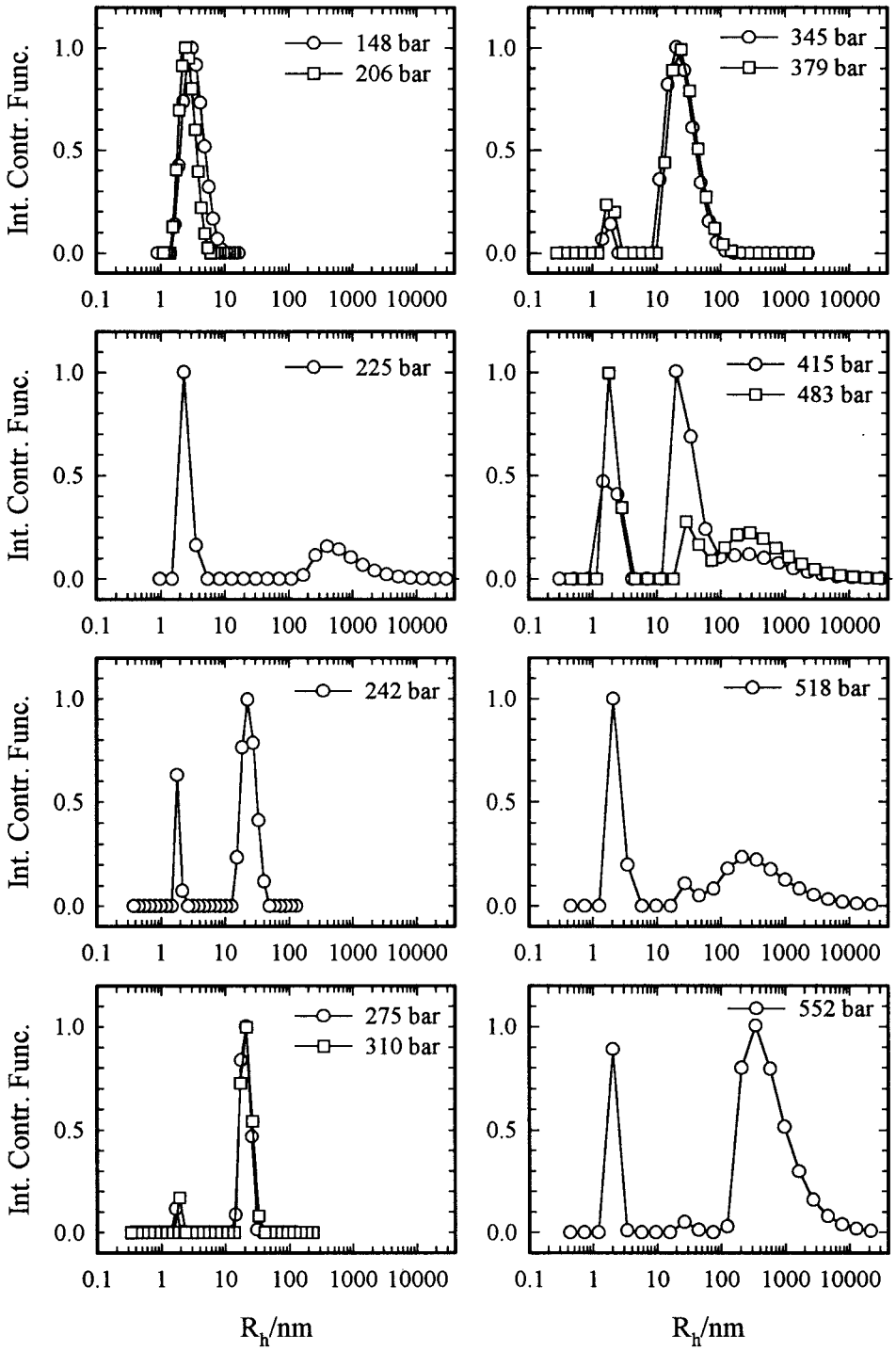

Figure 2. Intensity contribution function (i.e. $\Gamma G(\Gamma)$) vs (apparent) hydrodynamic radius R_h for the PFOA-*b*-PVAC copolymer solution in supercritical CO_2 at $C = 0.057$ g/mL, $T = 65$ °C, $\theta = 32°$ and indicated pressures. The peak area represents the scattered intensity contribution.

function is expressed in arbitrary unit, but normalized to the highest value at each pressure to facilitate comparisons. Therefore, the peak area is a measure of its scattering intensity contribution but on a relative scale. In comparison with Figure 1, the dynamic light scattering results can give us more important details about the pressure induced self-assembly behavior, such as the dynamic equilibrium between unimers and micelles (or large aggregates). With increasing pressure starting from 148 to 206 bar, narrowly distributed unimers with $\langle R_h \rangle$ of about 2.2 nm were first observed. When the pressure was increased to 225 bar, besides the narrow peak of unimers, polydisperse large aggregates with $\langle R_h \rangle$ of about 500 nm were detected. However, the two species made nearly the same contribution to the total scattered intensity. Assuming that approximately $M \propto R^3$ and the scattered intensity $I \propto CM$, the large aggregates could be estimated to take less than a few millionths of the polymer in weight fraction. Thus, the dominant species in the solution were still the dissolved unimers. By increasing the pressure to 242 bar, narrowly distributed micelles with $\langle R_h \rangle \sim 23$ nm were formed with an intensity ratio of micelles to unimers (I_m/I_u) of 6.2. A further increase of the pressure to 275 and 310 bar led to a dramatically increasing contribution of micelles to the total scattered intensity.

The I_m/I_u ratios were 30/1 and 20/1 at 275 and 310 bar, respectively. Moreover, the size distributions of the micelles were very narrow under the moderate pressures, i.e., with $\langle R_h \rangle$ of 20 nm and $\mu_2/\langle \Gamma \rangle^2$ of ~0.02. Two features could clearly be observed by further increasing the pressure from 345 to 552 bar. (1) The size distributions of micelles became broader toward the large R_h value until a large polydispersed aggregate peak appeared at 415 bar. (2) When the pressure was greater than 415 bar, with increasing pressure, the micelle peak became smaller and smaller, meanwhile, both the peak area of unimers and that of the large aggregates became bigger and bigger. On the basis of the assumption of $M \propto R^3$ and $I \propto CM$, the unimers in the solution were quantitatively overwhelming in the high-pressure region (> 415 bar). At 552 bar, the micelles were almost dissolved completely. Approximately, the pressure value of 552 bar can be taken as the critical micelle pressure (CMP) with $C = 0.057$ g/mL and $T = 65$ °C. Alternatively, we can consider the concentration of 0.057 g/mL as the cmc value at 552 bar and 65 °C.

As can be seen in Figure 2, the large aggregates appeared around the critical micelle pressure regions. This type of anomalous micellization process has been reported in the association behavior of various block copolymer systems induced by the temperature (or solvent composition) change.[12,14,37] The formation of the large aggregates has been ascribed to the composition heterogeneity of block copolymer. The chemical heterogeneity could be appreciable even for a copolymer with a narrow molar mass distribution. A small portion (i.e., only a few thousandths or so on a weight basis) of the copolymer specimen may exist with a higher content of the insoluble block. As the solvent quality becomes increasingly poorer by varying the temperature or the solvent composition, such minor components would become insoluble. For the PFOA-*b*-PVAC block copolymer in supercritical CO_2, when the pressure is high enough, the solvent is so good that all the copolymer chains can be soluble to form unimers. When the pressure is lowered, the minor less-soluble components prefer to precipitate out first, leading to the formation of a dilute dispersion of large colloidal particles stabilized by the adsorbed layer of the major component. When the pressure was further lowered to the CMP value of the major component, the insoluble minor components can either be incorporated into the micelle core or form mixed micelles. This is why three peaks were observed in the pressure region of 415−552 bar. By a further decrease in the pressure more and more micelles were formed so that all of the minor less-soluble components could go into the micellar core. Therefore, with decreasing pressure, the large aggregates disappeared gradually, and the size distribution of micelles became narrower and narrower until the pressure reached a value of 225 bar, where the micelles again disappeared, and some large aggregates were observed. In this regime, the large aggregates could also be interpreted by a similar principle. At such low pressures, the solvent quality is so poor that the phase separation pressure has been reached for the major component at the measured temperature. Therefore, the aggregates would precipitate from the solution. However, there may exist a small portion of the copolymer specimen having a higher content of the more-soluble block (i.e. PFOA), which can be adsorbed to the surface of major component to form some stable large colloidal particles. It should be noted that the critical phase separation pressure of ~225 bar for the PFOA-*b*-PVAC copolymer at 65 °C (CO_2 density ~0.72[36]) is in good agreement with the critical phase separation CO_2 density of 0.73 measured by NMR for PFOA at 64.6 °C.[38]

Figure 3 illustrates the similar association behavior in terms of the pressure dependence of the hydrodynamic radius distributions for the copolymer solution at a higher concentration of 0.096 g/mL at $\theta = 32°$ and $T = 65$ °C. A comparison between Figures 2 and 3 indicates that in the normal micelle region (242−310 bar) and the phase separation region (~225 bar), the self-assembly behavior is very similar for the two different concentration solutions. In the normal micellization region, both solutions showed a very narrow micelle peak with $\mu_2/\langle \Gamma \rangle^2$ of ~0.02 in equilibrium with unimers. The only difference is that the micelles make more contributions to the total scattered intensity with increasing concentration. However, in the high-pressure region, the dissolution of micelles was shifted to higher pressure with increasing concentration. Correspondingly, the appearance of large aggregates also shifted to higher pressures with increasing concentration. For example, the micelle peak in Figure 3 still takes ~25% of the total intensity contribution at 518 bar; in contrast, the micelles only contributed ~1% to the total scattered intensity in Figure 2. From a comparison between Figures 2 and 3 in the high-pressure region, we can conclude that the CMP values shift to higher pressures with increasing concentration. In other words, the higher the concentration of the solution, the higher the CMP.

Figure 4 shows the angular dependence of the hydrodynamic radius distributions of the copolymer solution with $C = 0.096$ g/mL at two different pressures: (a) 310 bar and (b) 518 bar. As discussed above, in the moderate pressure region, micelles made a major contribution to the scattered intensity. Thus, the minor less-soluble components of the copolymer could be incorporated into the CO_2-phobic micellar core and the spherical micelles with a CO_2-philic PFOA corona showed a very narrow distribution. No apparent angular dependence was expectedly observed for the size distributions of the micelles in a wide angular range of 32−146° at 310 bar. We also determined the concentration dependence of the translational diffusion coefficient of the spherical micelles in the normal micellar region (i.e. 275−310 bar).[39] The small positive diffusive second virial coefficient k_d of 3.2 mL/g at 275 bar and 65 °C indicated that the intermicellar interaction was slightly repulsive. The micelles showed a $\langle R_h \rangle_0$ value of 22 nm at infinite dilution under the conditions of 275 bar and 65 °C. However, in the anomalous micellization region (i.e. 518 bar), the broadly polydispersed large aggregates showed a strong angular dependence. The size of the large aggregates measured at high scattering angles was much smaller than those obtained at small scattering angles. By extrapolation to zero scattering angle, the large aggregates could be estimated to have an $\langle R_h \rangle$ value of about 250 nm. Although the CONTIN analysis for such a broadly polydispersed system could cause some uncertainty, the results clearly showed that the micelles with $\langle R_h \rangle \sim 12$ nm did not show an apparent angular dependence.

Critical Micelle Concentration. As shown in Figures 2 and 3, in the normal micellar region with moderate pressures (275−379 bar), the CONTIN results

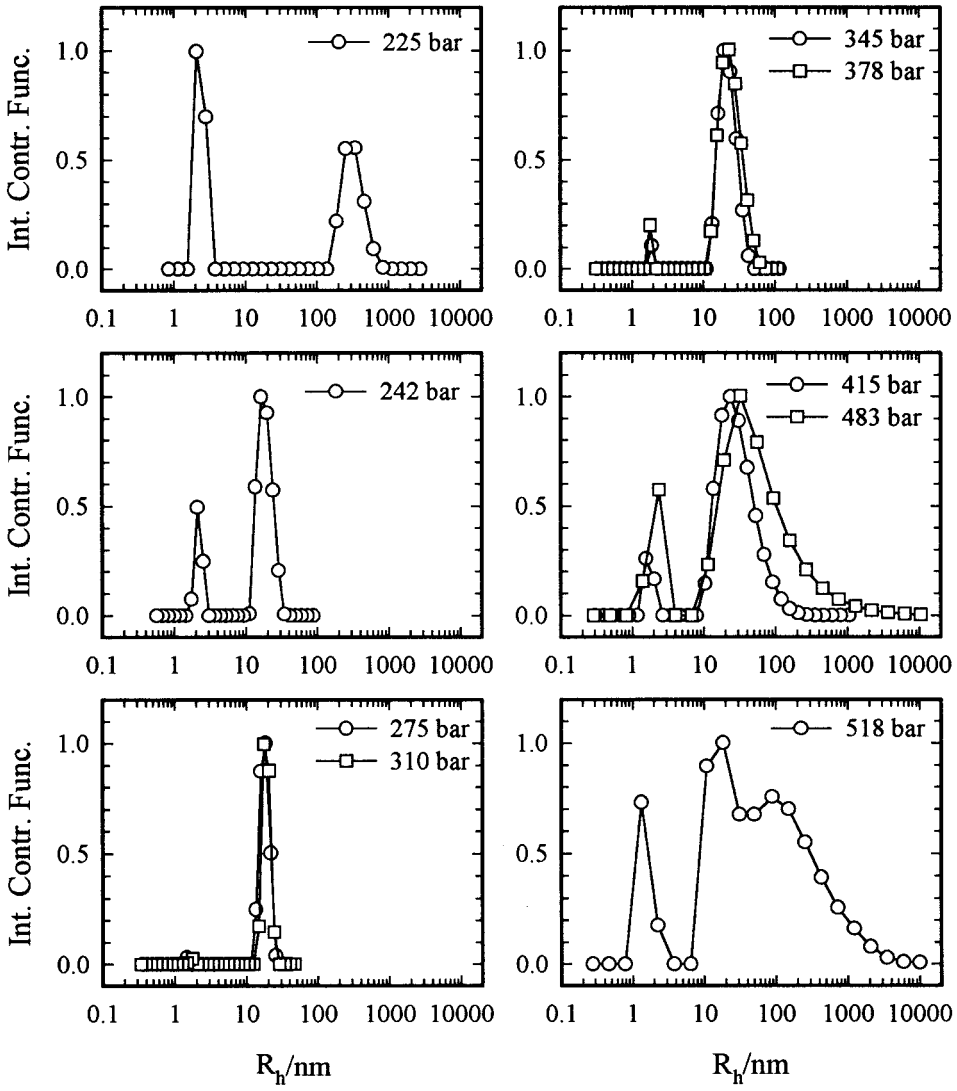

Figure 3. Intensity contribution function (i.e., $\Gamma G(\Gamma)$) vs (apparent) hydrodynamic radius R_h for the PFOA-*b*-PVAC copolymer solution in supercritical CO_2 at $C = 0.096$ g/mL, $T = 65$ °C, $\theta = 32°$, and the indicated pressures.

gave a bimodal size distribution. Moreover, both unimers and micelles were narrowly distributed. Therefore, it is possible to obtain some quantitative insights into the association behavior of the diblock copolymer in supercritical CO_2. Assuming that the solution is thermodynamically ideal and that the refractive index increment is approximately the same for both unimer and micelle species, the ratio of the relative intensity contributions made by micelles and unimers in the mixture can be further related to the concentration and molecular weight of each species by the expression

$$I_m/I_u \cong (C_m M_m)/(C_u M_u) \tag{5}$$

where C_m and C_u are, respectively, the concentration of micelles and that of unimers in solution and M_m and M_u are the molecular weight of micelles and unimers, respectively. According to the mass action law model of micelle formation, we may assume that the single micellar species with an aggregation number N is in equilibrium with the unimers. Therefore, $C_u = \text{cmc}$, $C_m = C - \text{cmc}$, and $N = M_m/M_u$ in an equilibrated solution containing a mixture of unimers and micelles. After the I_m/I_u values are obtained for two different concentrations but under the same temperature and pressure, the cmc can be calculated through eq 5. From the CONTIN results, the I_m/I_u values of 30/1, 20/1, 11/1, and 6.5/1 for the 0.057 g/mL solution, and of 63/1, 44/1, 26/1, and 17/1 for the 0.096 g/mL solution were obtained at 275, 310, 345, and 379 bar, respectively. The estimated cmc values together with the aggregation number N and the weight fraction for micelles at different pressures are listed in Table 1. With increasing pressure, the cmc increased and the aggregation number N decreased. This is understandable by considering the pressure-dependent solvent quality. As the pressure was increased, the solvent quality for both blocks became better, which decreased the selective solubility for the PFOA and PVAC blocks. To form micelles, more polymer surfactant needs to be added to the solution.

Figure 5 shows a plot of the logarithmic cmc against pressure. The open circles denote the results calculated from the CONTIN analysis, and the filled circle denote the CMP value measured directly from the pressure dependence of the hydrodynamic radius distributions with $C = 0.057$ g/mL. A plot of ln(cmc) vs pressure showed a very good linear relation with an expression

$$\ln(\text{cmc}) = 3.58 \times 10^{-3} P - 8.81 \tag{6}$$

However, the data calculated from the CONTIN analysis deviated from the linear plot with increasing

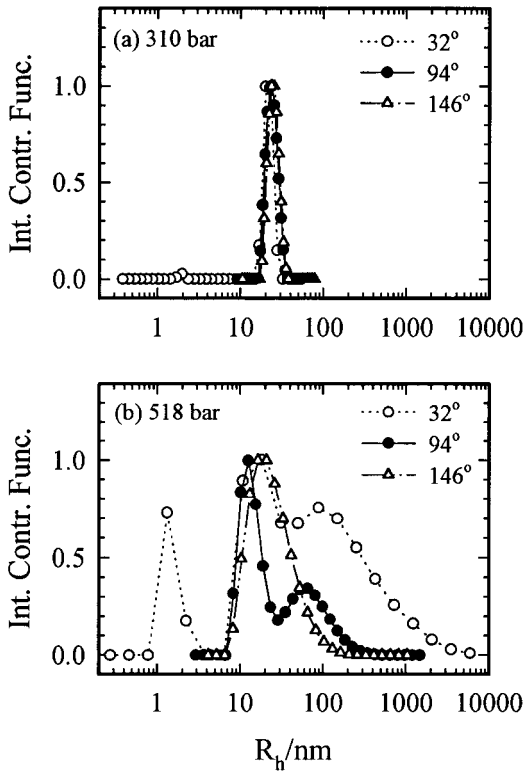

Figure 4. Angular dependence of the apparent hydrodynamic radius (R_h) distributions for the PFOA-*b*-PVAC copolymer solution in supercritical CO_2 at $C = 0.096$ g/mL, $T = 65$ °C, and two different pressures: (a) 310 bar, and (b) 518 bar.

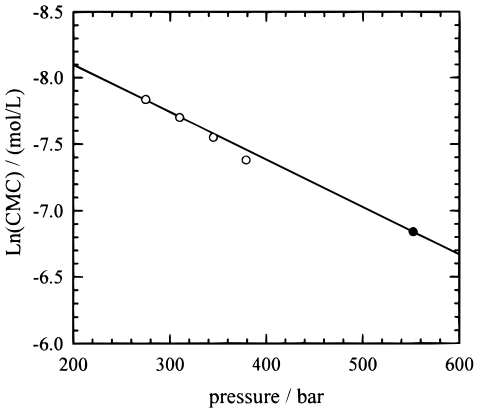

Figure 5. Plot of the logarithm of the critical micelle concentration (cmc) vs the measured pressure for the PFOA-*b*-PVAC copolymer solution in supercritical CO_2 at $T = 65$ °C.

pressure, i.e., at 379 bar. This deviation could be ascribed to the relatively broader size distributions of micelles and unimers at 379 bar, due to the appearance of a very small amount of anomalous large aggregates formed by the minor component of less-soluble copolymer specimen. The uncertainties associated with the CONTIN analysis for a broadly polydispersed system are not trivial. In the pressure region of 275−310 bar, both unimers and micelles showed a very narrow distribution. Thus, the uncertainties of the cmc values calculated from the CONTIN results could be very small in this pressure region.

As discussed above, the dynamic light scattering measurements in terms of the hydrodynamic radius distribution as a function of pressure give us a clearer vision on the pressure-induced micellization of block copolymer in supercritical CO_2. Besides the size and

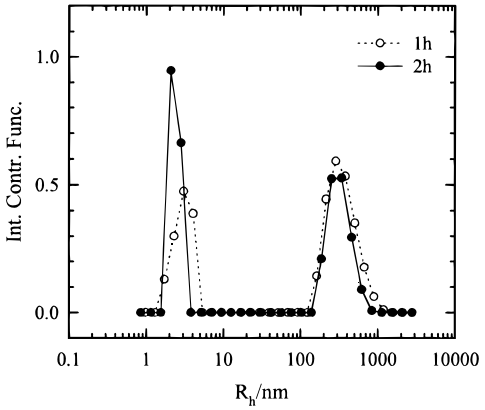

Figure 6. Time dependence of the hydrodynamic radius (R_h) distributions for the PFOA-*b*-PVAC copolymer solution in supercritical CO_2 at $C = 0.096$ g/mL, $\theta = 32°$, and $T = 65$ °C after the pressure was increased from 206 to 225 bar. The solution was stirred for 1 h, and then equilibrated for 15 min before collecting the data at $t = 1.5$ h.

Table 1. Micellar Properties of PFOA-*b*-PVAC Copolymer in Supercritical CO_2 at $T = 65$ °C

pressure, bar	*C*, g/mL	intensity ratio (micelle: unimer)	cmc, g/mL	N	wt fraction for micelles
275	0.057	30:1	0.021	18	0.62
	0.096	63:1			0.78
310	0.057	20:1	0.024	15	0.57
	0.096	44:1			0.75
345	0.057	11:1	0.028	11	0.50
	0.096	26:1			0.70
379	0.057	6.5:1	0.033	9	0.42
	0.096	17:1			0.65

size distribution for each species such as unimers, micelles, and large aggregates, dynamic light scattering can also give us the information about the cmc, aggregation number, and weight fraction for each species in solution. Although several assumptions have been made to simplify the calculation, Table 1 and Figure 5 can still provide us a deeper understanding on the association behavior of PFOA-*b*-PVAC copolymer in supercritical CO_2.

Dissolution Kinetics of the Copolymer. Figure 6 shows two hydrodynamic radius distributions for the PFOA-*b*-PVAC copolymer solution with $C = 0.096$ g/mL at $\theta = 32°$ and $T = 65$ °C, measured at two different time periods after the pressure was increased from 206 to 225 bar for 1.5 and 2.5 h, respectively. The solution was stirred for 1 h and then equilibrated for 15 min before collecting the data at $t = 1.5$ h. Two species with $\langle R_h \rangle$ of about 2.5 and 300 nm were observed, which could be attributed to the dissolved unimers and "undissolved" large aggregates. The $\langle R_h \rangle$ values of both the unimers and large aggregates remained nearly unchanged with increasing equilibration time from 1.5 to 2.5 h, however, the size distribution of both unimers and aggregates became narrower. Moreover, the narrowly distributed unimers ($\mu_2/\langle\Gamma\rangle^2 \sim 0.02$) made more contribution to the total scattered intensity with an increase in I_u/I_a from 0.5/1 to 0.9/1 after taking an additional hour for equilibration. Assuming $M \propto R^3$ and $I \propto CM$, the undissolved aggregates corresponded to about a few millionths fraction on a weight basis. Therefore, the unimers showed an overwhelming presence in the solution. This result, combined with the dramatic increase of the total scattered intensity of solution from 206 to 225 bar, as shown in Figure 1, indicates that nearly all of the copolymer could be dissolved to unimers at 225 bar and $T = 65$ °C.

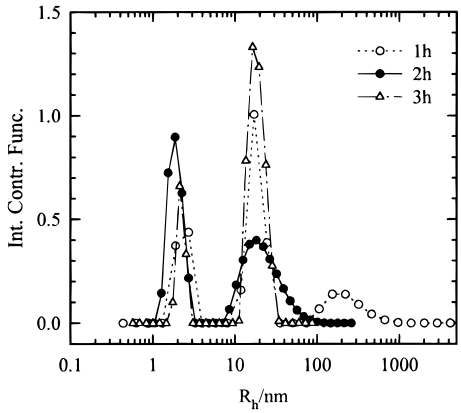

Figure 7. Typical micelle formation process in terms of the hydrodynamic radius R_h distributions for the PFOA-*b*-PVAC solution in supercritical CO_2 at $C = 0.096$ g/mL, $\theta = 32°$, and $T = 65$ °C after the pressure was increased from 225 to 242 bar. The solution was stirred for 30 min and then equilibrated for 20 min before collecting the data at $t = 1$ h.

Figure 7 shows the time dependence of the hydrodynamic radius distributions of PFOA-*b*-PVAC copolymer solution in supercritical CO_2 with $C = 0.096$ g/mL, $\theta = 32°$ and $T = 65$ °C after the pressure was increased from 225 to 242 bar. The solution was stirred for 30 min and then equilibrated for 20 min before collecting the data at $t = 1$ h. In comparison with Figure 6, during the first hour, the large undissolved aggregates were still detected, but the size and the intensity contribution of the large aggregates had decreased with increasing equilibration time. Meanwhile, a new species with $\langle R_h \rangle$ of about 18 nm appeared, which could be attributed to the micelles formed by the diblock copolymer of PFOA-*b*-PVAC in supercritical CO_2. During the second hour, the large aggregate peak disappeared completely; only unimers and micelles were observed. However, the hydrodynamic radius distributions of micelles were relatively broad, and the unimers still made a 50% contribution to the total scattered intensity. With further equilibration time, the size distribution of both unimers and micelles became narrower, while the micelle peak area became relatively large. The results measured at the third hour (denoted by hollow triangles) showed that after reaching the equilibrium, both unimers and micelles showed a very narrow size distribution with $\mu_2/\langle\Gamma\rangle^2$ of 0.018 and 0.04, respectively. The unimers have only an ~15% contribution to the total scattered intensity at 242 bar. To be sure that the process of stirring did not kick up some insoluble fractions that gradually settled out of solution, we had stirred the solution again after it was settled for overnight. The measured R_h distribution remained unchanged in comparison with the results obtained at the third hour, after the stirring was stopped. The experimental results in Figures 6 and 7 indicate that the process of dissolution and micelle formation for the PFOA-*b*-PVAC copolymer in supercritical CO_2 was relatively slow at pressures just above the phase separation pressure regime, i.e., taking several hours to reach the equilibrium state.

Conclusions

Light-scattering results at 65 °C for the PFOA-*b*-PVAC diblock copolymer in supercritical CO_2, a pressure-dependent selective good solvent for the PFOA block, permit us to draw the following conclusions. (1) micelles with a starlike structure having the PVAC block in the core and the PFOA block in the corona can be induced by changing pressures. Five regions appear in sequence with increasing pressure. At very low pressures (<148 bar), the block copolymer was insoluble. At low pressures (148−206 bar), a small portion of the copolymer could be dissolved to form unimers. Around the phase separation pressure of the block copolymer (~225 bar), large aggregates were formed together with dissolved unimers. At moderate pressures of 242−310 bar, very narrowly distributed micelles without apparent angular dependence were formed. At high pressures, micelles were broken up to unimers gradually with increasing pressure. Meanwhile, micelles showed a broader distribution toward the larger size and eventually led to the appearance of large polydisperse aggregates around the critical micelle pressure. (2) Similar to some types of block copolymers in a selective solvent, the composition heterogeneity of the fluorinated copolymer could also cause complex states of aggregation in supercritical CO_2. (3) Some quantitative (or semiquantitative) information on the molecular association behavior could be extracted from the CONTIN analysis in the normal micellization pressure region with narrow size distributions for both unimers and micelles. With increasing pressure, the critical micelle concentration increased, but the aggregation number of micelles decreased. (4) Both the dissolution and the micelle formation of the diblock copolymer showed a slow kinetic process, i.e., taking several hours to reach equilibrium.

Acknowledgment. B.C. gratefully acknowledges the support of this work by the U.S. Department of Energy (DEFG0286ER45237.013). He also wishes to thank the National Science Foundation (INT-9515361) for starting the project, the Du Pont Company for an unrestricted grant for laser repair, and Professor J. M. DeSimone, at the University of North Carolina at Chapel Hill, for a sample of the PFOA-*b*-PVAC diblock copolymer.

References and Notes

(1) DeSimone, J. M.; Guan, Z.; Elsbernd, C. S. *Science* **1992**, *257*, 945.
(2) Kiran, E.; Levelt Sengers, J. M. H. Eds. *Supercritical Fluids: Fundamentals for Applications*; Kluwer: Dordrecht, The Netherlands, 1994.
(3) Kaiser, J. *Science* **1996**, *274*, 2013.
(4) Black, H. *Environ. Sci. Technol.* **1996**, *30*, 125A.
(5) Johnston, K. P.; Harrison, K. L.; Clarke, M. J. Howdle, S. M.; Heitz, M. P.; Bright, F. V.; Clarlier, C.; Randolph, T. W. *Science* **1996**, *271*, 624.
(6) McHugh, M. A.; Krukonis, V. *J. Supercritical Fluid Extraction-Principles and Practice*: Butterworth: Boston, MA, 1986.
(7) Guan, Z.; DeSimone, J. M. *Macromolecules* **1994**, *27*, 5527.
(8) Canelas, D. A.; Betts, D. E.; DeSimone, J. M. *Macromolecules* **1996**, *29*, 2818.
(9) McClain, J. B.; Londono, D.; Combes, J. R.; Romack, T. J.; Canelas, D. A.; Betts, D. E.; Wignall, G. D.; Samulski, E. T.; DeSimone, J. M. *J. Am. Chem. Soc.* **1996**, *118*, 917.
(10) Hyatt, J. A. *J. Org. Chem.* **1984**, *49*, 5097.
(11) Zhou, Z.; Chu, B. *J. Colloid Interface Sci.* **1988**, *126*, 171.
(12) Zhou, Z.; Chu, B. *Macromolecules* **1988**, *21*, 2548.
(13) Zhou, Z.; Chu, B.; Peiffer, D. G. *Macromolecules* **1993**, *26*, 1876.
(14) Zhou, Z.; Chu, B.; Peiffer, D. G. *Langmuir* **1995**, *11*, 1956.
(15) Zhou, Z.; Chu, B.; Nace, V. M. *Langmuir* **1996**, *12*, 5016.
(16) Ritter, J. M.; Palavvra, A. M. F.; Kao, C. P. C.; Paulaitis, M. E. *Fluid Phase Equilib.* 1990, *55*, 173.
(17) Kaler, E. W.; Billman, J. F.; Fulton, J. L.; Smith R. D. *J. Phys. Chem.* **1991**, *95*, 458.

(18) Zielinski, R. G.; Paulaitis, M. E.; Kaler, E. W. *Rev. Sci. Instrum.* **1996**, *67*, 2612.
(19) Fulton, J. L.; Pfund, D. M. In *Proceedings of Third International Symposium on Supercritical Fluids*; Perrut Ed.: Strasburg, France, 1994; p 391.
(20) Fulton, J. L.; Pfund, D. M.; Smith, R. D.; Carnaham, N. F.; Quintero, L.; Capel, M.; Leontaritis, K. *Langmuir* **1993**, *9*, 2035.
(21) Fulton, J. L.; Pfund, D. M.; McClain, J. B.; Romack, T. J.; Maury, E. E.; Combes, J. R.; Samulski, E.; deSimone, J. M.; Capel, M. *Langmuir* **1995**, *11*, 4241.
(22) Chillura-Martino, D.; Triolo, R.; McClain, J. B.; Combes, J. R.; Betts, D. E.; Canelas, D. A.; DeSimone, J. M.; Samulski, E. T.; Cochran, H. D.; Londono, J. D.; Wignall, G. D. *J. Mol. Struct.* **1996**, *383*, 3.
(23) McClain, J. B.; Betts, D. E.; Canels, D. A.; Samulski, E. T.; DeSimone, J. M.; Londono, J. D.; Cochran, H. D.; Wignall, G. D.; Chillura-Martino, D.; Triolo, R. *Science* **1996**, *274*, 2049.
(24) Fulton, J. L.; Blitz, J. P.; Tingey, J. M.; Smith, R. D. *J. Phys. Chem.* **1989**, *93*, 4189.
(25) Smith, R. D.; Fulton, J. L.; Blitz, J. P.; Tingey, J. M. *J. Phys. Chem.* **1990**, *94*, 781.
(26) Beckman, E. J.; Smith, R. D. *J. Phys. Chem.* **1990**, *94*, 3729.
(27) Kojima, J.; Takenaka, M.; Nakayama, Y.; Hashimoto, T. *Rev. Sci. Instrum.* **1995**, *66*, 4066.
(28) Zhou, S. Q.; Chu, B.; Dhadwal, H. S. *Rev. Sci. Instrum.* **1998**, *69*, 1955.
(29) Dhadwal, H. S.; Chu, B. *Rev. Sci. Instrum.* **1984**, *60*, 845.
(30) Betts, D.; Johnson, T.; Anderson, C.; DeSimone, J. M. *Polym. Prepr. (Am. Chem. Soc. Div. Polym. Chem.)* **1997**, *38*, 760.
(31) Provencher, S. W.; *Makromol. Chem.* **1979**, *180*, 201; *Comput. Phys. Commun.* **1982**, *27*, 213.
(32) Pecora, R. *Dynamic Light Scattering*, Plenum Press: New York, 1976.
(33) Chu, B. *Laser Light Scattering*, 2nd ed.; Academic Press: New York, 1991.
(34) Stephan, K.; Lucas, K. *Viscosity of Dense Fluids*; Plenum Press: New York, 1979.
(35) Besserer, G. J.; Robinson, D. B. *J. Chem. Eng. Data*, **1973**, *18*, 137.
(36) Angus, S.; Armstrong, B.; DeReuck, K. M. *International Thermodynamic Tables of the Fluid State*: *Carbon Dioxide*, *IUPAC*; Pergamon Press: New York, 1976.
(37) Brown, W.; Schillen, K.; Almgren, M.; Hvidt, S.; Bahadur, P. *J. Phys. Chem.* **1991**, *95*, 1850.
(38) Dardin, A.; Cain, J. B.; DeSimone, J. M.; Johnson, C. S., Jr.; Samulski, E. T. *Macromolecules* **1997**, *30*, 3593.
(39) Zhou, S. Q.; Chu, B. *Macromolecules*, in press.

MA980262+